



# The effect of electron scattering from disordered grain boundaries on the resistivity of metallic nanostructures



Claudio Arenas<sup>a,b</sup>, Ricardo Henriquez<sup>c</sup>, Luis Moraga<sup>d</sup>, Enrique Muñoz<sup>e</sup>, Raul C. Munoz<sup>a,\*</sup>

<sup>a</sup> Departamento de Física, Facultad de Ciencias Físicas y Matemáticas, Universidad de Chile, Blanco Encalada 2008, Casilla 487-3, Santiago 8370449, Chile

<sup>b</sup> Synopsys Inc., Avenida Vitacura 5250, Oficina 708, Vitacura, Santiago, Chile

<sup>c</sup> Departamento de Física, Universidad Técnica Federico Santa María, Av. España 1680, Casilla 110-V, Valparaíso, Chile

<sup>d</sup> Universidad Central de Chile, Toesca 1783, Santiago, Chile

<sup>e</sup> Facultad de Física, Pontificia Universidad Católica de Chile, Casilla 306, Santiago 7820436, Chile

## ARTICLE INFO

### Article history:

Received 12 August 2014

Received in revised form 9 November 2014

Accepted 8 December 2014

Available online 15 December 2014

### PACS:

73.50.–h

73.61.–r

### Keywords:

Resistivity of thin metallic nanostructures  
Quantum theory of electron grain boundary scattering

Green's function and Kubo linear response theory

Kronig–Penney potential

Anderson localization

## ABSTRACT

We calculate the electrical resistivity of a metallic specimen, under the combined effects of electron scattering by impurities, grain boundaries, and rough surfaces limiting the film, using a quantum theory based upon the Kubo formalism. Grain boundaries are represented by a one-dimensional periodic array of Dirac delta functions separated by a distance “ $d$ ” giving rise to a Kronig–Penney (KP) potential. We use the Green's function built from the wave functions that are solutions of this KP potential; disorder is included by incorporating into the theory the probability that an electron is transmitted through several successive grain boundaries. We apply this new theory to analyze the resistivity of samples S1, S2, S7 and S8 measured between 4 and 300 K reported in *Appl. Surf. Science* **273**, 315 (2013). Although both the classical and the quantum theories predict a resistivity that agrees with experimental data to within a few percent or better, the phenomena giving rise to the increase of resistivity over the bulk are remarkably different. Classically, each grain boundary contributes to the electrical resistance by reflecting a certain fraction of the incoming electrons. In the quantum description, there are states (in the allowed KP bands) that transmit electrons unhindered, without reflections, while the electrons in the forbidden KP bands are localized. A distinctive feature of the quantum theory is that it provides a description of the temperature dependence of the resistivity where the contribution to the resistivity originating on electron–grain boundary scattering can be identified by a certain unique grain boundary reflectivity  $R$ , and the resistivity arising from electron–impurity scattering can be identified by a certain unique  $\ell_{\text{IMP}}$  mean free path attributable to impurity scattering. This is in contrast to the classical theory of Mayadas and Shatzkes (MS), that does not discriminate properly between a resistivity arising from electron–grain boundary scattering and that arising from electron–impurity scattering, for MS theory does not allow parameters ( $\ell_{\text{IMP}}$ ,  $R$ ) to be uniquely adjusted to describe the temperature dependence of the resistivity data. The same data can be described using different sets of ( $R$ ,  $\ell_{\text{IMP}}$ ); the latter parameter can be varied by two orders of magnitude in the case of small grained samples  $d < \ell$ , and by a factor of 4 in the case of samples made out of large grains  $d > \ell$  (where  $\ell$  is the bulk mean free path at 300 K). For samples  $d > \ell$ , the increase of resistivity is attributed not to electrons being partially reflected by the grain boundaries, but to a decrease in the number of states at the Fermi sphere that are allowed bands of the KP potential; hence the reflectivity required by the quantum model turns out to be an order of magnitude smaller than that required by the classical MS theory. For samples  $d < \ell$ , the resistivity increase originates mainly from Anderson localization induced by electron grain boundary scattering from disordered successive grains characterized by a localization length of the order of 110 nm and not from electrons being partially reflected by grain boundaries; the outcome is that the reflectivity required by the quantum theory turns out to be about 4 times smaller than that required by the classical MS theory.

© 2014 Elsevier B.V. All rights reserved.

\* Corresponding author. Tel.: +56 2 2978 4335.

E-mail address: [ramunoz@ing.uchile.cl](mailto:ramunoz@ing.uchile.cl) (R.C. Munoz).

## 1. Introduction

Progress in the manufacturing of integrated circuits has led to a decrease of the linear dimensions of connecting lines, such that the width of interconnects is now comparable to or smaller than the electron mean free path in the bulk at 300 K (39 nm in Cu), and the wire width is rapidly approaching dimensions which are about an order of magnitude larger than the electronic Fermi wave length. At these short scales quantum effects are expected to dominate charge transport. Hence, a quantum description of the increase in resistivity arising from electron scattering by grain boundaries and rough surfaces (over and above the resistivity of the bulk) is necessary. In this paper we present such a quantum theory.

Fuchs [1] and Sondheimer [2] (FS) published a description of size effects on thin metallic films based upon a solution of the Boltzmann Transport Equation (BTE). However, measurements of the resistivity on thin films of increased purity revealed that as the film thickness shrinks, the resistivity increases beyond the FS predictions. Mayadas and Shatzkes (MS) attributed this additional increase of resistivity to electron scattering by grain boundaries; they developed a theory that includes electron scattering by both rough surfaces and by grain boundaries, that is also based upon a solution of BTE [3].

When solving BTE, the effects of scattering by phonons/distributed impurities is accounted for by the time of relaxation  $\tau$ , while rough surface scattering is accounted for by choosing appropriate boundary conditions. Grain boundary scattering is represented in MS theory by a Boltzmann collision integral including a transition probability calculated by first-order perturbation theory, where the unperturbed electron states are plane waves and the perturbation Hamiltonian is a series of delta function potentials equally spaced, oriented perpendicular to the electric field [3].

Experimental research published recently, and theoretical results published over decades raise fundamental questions regarding the classical MS formalism, in spite of its wide spread use in microelectronics.

From the experimental side, the resistivity between 4 and 300 K has been reported, as well as the Hall effect measured between 4 and 50 K. These transport measurements were performed in specimens where grain size and surface roughness were no longer considered as adjustable parameters, but were determined instead via independent STM and TEM experiments performed on each sample [4–9], and grain size as well as film thickness were varied independently. It turns out that when the gold films are made out of columnar grains (extending from the bottom to the top of the film), and when  $d > t$  (where  $d$  is the average grain diameter and  $t$  the film thickness), the Hall mobility  $\mu_H$  (4) at 4 K increases linearly with  $t$ . However, when  $d < t$ ,  $\mu_H$  (4) increases linearly with grain diameter  $d$  regardless of film thickness [5]. Borrowing arguments from the theory of mobility of electrons in solids [10], *this linear dependence of  $\mu_H$  on  $d$  or  $t$  allows the univocal identification of whether the dominant electron scattering mechanism at 4 K is electron-grain boundary or electron-surface scattering, respectively.* If resistivity data are analyzed following MS theory, *then in films where  $d \approx 12$  nm, the increase in resistivity at 4 K (where electron-grain boundary scattering is dominant) turns out to be about two orders of magnitude (Fig. 3 in Ref. [4]).* It is quite doubtful that an increase in resistivity larger than one, of the order of a factor 100, could be correctly described by a formalism based upon first order perturbation theory.

Moreover, evidence pointing to the failure of semi classical models to describe the resistivity of nanometric polycrystalline tungsten films has recently been published by Choi et al.; in

this work the authors state explicitly that “...first principle methods based on Green’s functions approaches represent an important way forward toward developing more predictive models” [11].

From the theoretical side, Monte Carlo simulations of the electrical conduction in thin polycrystalline metallic films has recently been published by Rickman and Barmack; the results suggest that microstructure plays an important role (not included in the classical phenomenological model of Mayadas and Shatzkes), leading to a conductivity that can be described in limiting cases in terms of either a simplified trapping model or a hopping model [12].

Another aspect that seems questionable in MS theory, is that the solution of BTE in the presence of scattering in the bulk ( $B$ ) characterized by a relaxation time  $\tau$ , and grain boundary scattering (GB), can be described by an effective relaxation time  $\tau^*$  given by Eq. (7b) from Ref. [3], analogous to Mathiessen’s rule, which leads to Eq. (8) from Ref. [3], for the conductivity of a specimen where both electron scattering processes are present. Hence, the authors assume that the resistivity observed when both electron scattering processes ( $B$ ) and (GB) are present, do not interfere with each other. Although a quantum theory of electron-grain boundary scattering has not emerged yet, several quantum theories describing electron scattering in the bulk and electron-rough surface scattering have been published. Theoretical calculations recently published [13,14], as well as experimental evidence on CoSi<sub>2</sub> films, suggest that the correct quantum description of charge transport leads to interference between electron scattering in the bulk and electron-rough surface scattering when both electron scattering mechanisms are present; such interference gives rise to severe violations of Mathiessen’s rule in nanometric metallic structures [15]. A similar interference between electron scattering in the bulk and electron-grain boundary scattering leading to severe violations of Mathiessen’s rule may be expected from a quantum description of charge transport; this will be addressed to below.

Perhaps the most severe criticism to MS theory is that it does not seem consistent with Bloch’s theorem. On the one hand, Bloch’s solutions of the Schrödinger equation describing an electron in a periodic potential  $V_0(\mathbf{r}) = V_0(\mathbf{r} + \boldsymbol{\rho})$  are known to exhibit the periodicity  $\boldsymbol{\rho}$  of the lattice potential  $V_0(\mathbf{r})$ , and hence extend throughout the crystal. On the other hand, the MS formalism includes the effect of *columnar grain boundaries* by means of another *periodic potential made up of a series of uniform, equally spaced delta functions*. MS calculated the conductivity of this crystal containing a periodic array of grain boundaries assuming that at each grain boundary, a fraction  $0 < R < 1$  of the electrons (represented by plane waves) colliding with each one of these grain boundaries is specularly reflected. Hence electrons colliding with individual, periodically distributed grain boundaries are assumed to be partially reflected and all grains are assumed to be endowed with the same reflectivity  $R$ ; but yet, *electrons colliding with individual, periodically distributed ions making up the crystalline lattice do not undergo such reflection.*

The key to clear this confusion and to elucidate the physics underlying the increase in resistivity (over the bulk) induced by grain boundaries, resides in realizing that the allowed states of the periodic potential representing equally spaced grains are also extended throughout the crystal. These Bloch states extending throughout the crystal (containing equally spaced grains) were taken for granted in the original paper by Mayadas and Shatzkes, for they state explicitly that “...in the limit  $s \rightarrow 0$ ,  $\sigma_G \rightarrow \sigma_0$ , and thus a periodic arrange of planes provides no resistance” (over and above the resistance of the bulk) [Ref. [3], p. 1384]. Hence the increase in resistivity arises primarily because grain boundaries are *not equally spaced but are randomly distributed; consequently, electron*

transmission through disordered grains should play a central role in the theory. Since the work of Anderson and others [16–18], we know that the solutions of the Schrödinger equation in a randomly varying potential in  $1-D$  are no longer extended but are localized. In the words of Anderson, “. . . at sufficiently low densities. . . transport does not take place; the exact wave functions are localized in small regions of space” [16]. Moreover, in Chapter 2 of Ref. [18] (p. 7), Thouless states that “. . . In a weakly disordered one-dimensional potential, all states are localized”. The effect of these localized states on the resistance of metallic wires at very low temperatures, in the words of Thouless, leads to “. . . the resistance should increase exponentially with length instead of linearly” [17].

In the MS model the role of disorder is minimal, for the calculation of the probability of electron transmission through consecutive (disordered) grain boundaries – the core of a proper theory describing the physics that gives rise to the increase of resistivity induced by electron-grain boundary scattering – is missing, it is entirely omitted from the theory. In the quantum model described below electron transmission through consecutive grains plays a key role.

In this paper we calculate the electrical resistivity of a metallic specimen under the combined effects of electron scattering by impurities, grain boundaries, phonons and a rough surface limiting the film, using the standard method based upon the Kubo formalism. Grain boundaries are represented by a one-dimensional periodic array of Dirac delta functions giving rise to a Kronig–Penney (KP) potential; to compute the conductivity we use the Green’s function built from the wave functions that are solutions of this KP potential. However, a quantum description of the resistivity of metallic specimens could be considered an interesting and challenging exercise of Mathematical Physics of little practical use, unless the predictions of the model are compared with resistivity data to assess its predictive power, and the predictions of the classical model are compared with the predictions of the quantum theory. Hence, we apply this new theory (as well as the MS theory) to analyze data on samples where the temperature dependence of the resistivity between 4 and 300 K has been reported, as well as a full, systematic characterization of surface roughness and grain size distribution has been measured independently and has been published for each sample: We analyze the data from samples S1, S2, S7 and S8 in Ref. [4].

The paper is organized as follows. In Section 2 we present the outline of the classical result obtained by Mayadas and Shatzkes, as well as the outline of the new quantum theory. For easy reading we include in the Appendix a number of laborious mathematical details, and include in Section 2 only the essential building blocks of the new theory. We stress at the outset that Anderson localization is *not one of the starting assumptions of this paper*. Quite to the contrary, we spent some time trying to develop a quantum theory of electron-grain boundary scattering using the standard tools of an introductory course on Quantum Mechanics. Rather to our surprise, as discussed in detail in Appendix D, the results forced us to admit that the numerical evaluation of the average of the matrix describing electron transmission through  $N$  consecutive (disordered) grain boundaries, was consistent with Anderson localization phenomena.

After Section 2 we do not include a Section describing surface characterization and experimental methodology, for this has already been published in Section 2 of Ref. [4]. Instead, in Section 3 we outline some relevant conceptual aspects of the new quantum theory that are at variance with the classical MS theory, and describe the results of the data analysis. In Section 4, we discuss the results of comparing the predictions of the classical theory with the temperature dependence of the resistivity on Samples S1, S2, S7 and S8 from Ref. [4], and with the predictions of the new quantum theory. In Section 5, we summarize the main

conclusions of this work and the practical applications deriving from it.

## 2. Theory

### 2.1. Classical theory: Mayadas and Shatzkes

For a thin film bounded by two different surfaces, the Mayadas and Shatzkes theory yields  $\rho/\rho_0 = f(\ell_0(T), d, s, P, Q, R, t)$  [4]:

$$\left(\frac{\rho_0}{\rho}\right) = \frac{3}{2} \int_{-1}^1 \frac{\tau^*(u, d, s)}{\tau} u^2 du - \frac{3\ell_0}{4t} \int_0^{2\pi} \int_0^{\pi/2} \left(\frac{\tau^*(\zeta, d, s)}{\tau}\right)^2 \times \frac{\cos^2(\phi) \sin^3(\theta) [1 - E(\zeta)] [2 - P - Q + (P + Q - 2PQ)E(\zeta)]}{1 - PQE(\zeta)^2} d\theta d\phi \quad (1)$$

with  $u = \cos(\theta)$ ,  $\zeta = \sin(\theta)\cos(\phi)$ ,  $E(\zeta) = \exp\left(-\frac{t}{v_F \tau^*(\zeta, d, s) \cos(\theta)}\right)$  and

$$\frac{1}{\tau^*(\zeta, d, s)} = \frac{1}{\tau} + \frac{\ell_0}{d} \frac{R}{1-R} \frac{1}{\tau\zeta} \frac{1 - \exp(-4(\zeta k_F)^2 s^2)}{1} \times \frac{1}{1 - 2 \exp(-2(\zeta k_F)^2 s^2) \cos(2\zeta k_F d) + \exp(-4(\zeta k_F)^2 s^2)}$$

where  $\rho(T)$  is the resistivity of the film,  $\rho_0(T)$  is the resistivity of the bulk (a fictitious crystalline sample of the same thickness  $t$  but without grains, carrying the same concentration of impurities/point defects as the thin film, but limited by two atomically flat surfaces),  $\tau(T)$  is the average electronic collision time describing electron scattering in the bulk,  $\ell_0(T)$  is the (unknown) electronic mean free path in the bulk at temperature  $T$ ,  $d$  and  $s$  are the average grain diameter and standard deviation characterizing the Gaussian distribution of grain sizes, respectively.  $P$  and  $Q$  are the reflectivity of the two surfaces limiting the film,  $R$  is the reflectivity coefficient characterizing each grain boundary and  $k_F$  is the Fermi wave vector.

### 2.2. Quantum theory

We outline below the fundamentals of the new quantum theory.

#### 2.2.1. Kubo’s formalism

We start with the electronic wave functions corresponding to the solution of the Schrödinger equation in a periodic potential  $V(\mathbf{r})$  representing the grain boundaries, given by

$$V(\mathbf{r}) = V(x) = \sum_{n=-N/2}^{N/2} \left(\frac{\hbar^2 S}{2m}\right) \delta(x - nd) \quad (2)$$

In the limit when  $N$  tends to infinity, this is the Kronig–Penney (KP) potential [19].

To compute the conductivity  $\sigma$  we use the Kubo formalism [20]. In a somewhat simplified form, it leads to [21,22]

$$\sigma = -\frac{2q^2 \hbar^3}{\pi m^2 \Omega} \int d^3 \vec{r} \int d^3 \vec{r}' \left[ \Im m \frac{\partial G(\vec{r}, \vec{r}')}{\partial x} \right] \left[ \Im m \frac{\partial G(\vec{r}', \vec{r})}{\partial x'} \right] \quad (3)$$

where  $q$  and  $m$  are the charge and effective mass of the carriers,  $\Omega$  is the volume of the sample and  $G(r, r')$  is Green’s function appropriate for the KP potential described by Eq. (2);  $\Im m(z)$  represents the imaginary part of the complex number  $z$ . As discussed in Appendix B, to account for dissipation deriving from electron scattering by phonons/distributed impurities, an imaginary part is added to the Fermi energy – or to the Fermi wave vector  $k_F$  – as the quantum analogue of the mean free path  $\ell$ , so we define  $k_F = k_F + (i/2\ell)$  [23,24].

2.2.2. Green's function for the Kronig–Penney potential

As shown in Appendix A, the Green's function  $g(k, x, x')$  for the Kronig–Penney potential is

$$g(k; x, x') = \frac{\phi(-\xi, x)\phi(\xi, x')}{2ik \sin(kd) \sin \xi} \quad \text{if } x < x'$$

$$g(k; x, x') = \frac{\phi(-\xi, x')\phi(\xi, x)}{2ik \sin(kd) \sin \xi} \quad \text{if } x > x'$$

where  $\phi(x) = \sum_{m=-\infty}^{\infty} \theta_m(x) \exp(im\xi)u(x - md)$  with  $u(x) = \sin[k(x - d)] + \exp(i\xi)\sin[kx]$  and  $\theta_m = 1$  if  $md \leq x \leq (m + 1)d$  and zero otherwise, so instead of the plane waves used by MS along  $x$ , we use  $\phi(x) = \sum_{m=-\infty}^{\infty} \theta_m(x) \exp(im\xi)\{\sin[k(x - (m + 1)d)] - \exp(i\xi)\sin[k(x - md)]\}$ .

In order that  $\phi(x)$  be an eigenfunction of the potential described by Eq. (2), the relationship between  $k$  and the Kronig–Penney parameter  $\xi$  is through the KP function  $f_{KP}(S, d, u)$ :

$$f_{KP}(S, d, u) = \cos \xi = \cos(u) + \frac{Sd \sin(u)}{2u} \quad (4)$$

where  $u = k \cdot d$ . In this relation  $k$  is a complex number, and so is  $\xi$ . We choose  $\sin(\xi)$  such that  $|\cos(\xi) + i \sin(\xi)|^2 \leq 1$ .

In the case of the bulk crystal plus the Kronig–Penney potential (2), the wave function  $\Psi(x, y, z)$  satisfying the Schrödinger equation, may be written as  $\Psi(x, y, z) = \phi(x)f(y, z)$ , where  $f(y, z)$  should be plane waves with  $k^2 = k_F^2 - k_\perp^2$ ,  $\mathbf{r}_\perp = \mathbf{y}\mathbf{y} + \mathbf{z}\mathbf{z}$ ,  $\mathbf{k}_\perp = k_y\mathbf{y} + k_z\mathbf{z}$  (where  $\mathbf{y}$  and  $\mathbf{z}$  are unit vectors along  $y$  and  $z$ , respectively).

To compare the predictions of the present theory with the classical predictions, we need to relate the reflectivity  $R$  of one grain introduced by MS, with the strength of the delta function  $S$  appearing in Eqs. (2) and (4). We follow Mayadas and Shatzkes and note that reflection coefficient  $R$  of a single barrier  $(\hbar^2 S/2m) \delta(x - x_0)$  is related to  $S$  by  $R = S^2/(S^2 + 4k_x^2)$ . To obtain the same reflectivity  $R$  for all grain boundaries (as required by MS theory), we set  $k_x = k_F$ .

2.2.3. Conductivity of a crystalline sample containing uniform, equally spaced grains

As shown in Appendix B, the electrical conductivity of a crystalline sample containing uniform, equally spaced grains predicted by theory is

$$\sigma = \frac{q^2}{8\pi^2 \hbar} \int_0^\infty \frac{I(k)}{|D(k)|^2} T_N(k_x) k_\perp dk_\perp \quad (5)$$

where  $D(k) = k \sin(kd) \sin(\xi)$ , with  $k = \sqrt{\tilde{k}_F^2 - k_\perp^2}$  (a complex quantity due to the renormalization of  $k_F$ ) and  $k_x = \sqrt{k_F^2 - k_\perp^2}$ . Also:

$$I(k) = I_A(k) + I_B(k) + I_C(k) \quad (5a)$$

with

$$I_A(k) = \sinh(2\xi_I) \left[ \frac{k_R^2}{k_I} \sinh(2k_I d) - \frac{k_I^2}{k_R} \sin(2k_R d) \right] - \sin(2\xi_R) \left[ \frac{k_R^2}{k_I} \sin(2k_R d) + \frac{k_I^2}{k_R} \sinh(2k_I d) \right] \quad (5b)$$

$$I_B(k) = \frac{1}{d} [\cos(2k_R d) - \cosh(2k_I d)] \left[ \frac{k_R^2 - k_I^2}{k_R^2 + k_I^2} \sinh(2\xi_I) + \frac{2k_R k_I}{k_R^2 + k_I^2} \sin(2\xi_R) \right] \quad (5c)$$

$$I_C(k) = 4\Im \left\{ \sin(\xi) \left[ i \frac{k_R^2}{k_I} + \frac{k_I^2}{k_R} \right] \sin(kd) \right\} + \frac{2}{d} \Im \left[ \frac{k}{k^*} \sin(\xi) \sin(2k * d) \sin(kd) \right] \quad (5d)$$

where the coefficient  $T_N(k_x)$  has been introduced to represent the probability that an electron will be transmitted through  $N$  successive grain boundaries perpendicular to  $x$  ( $T_N = 1$  if all grain boundaries are equally spaced). Here  $k_R$  and  $k_I$  are the real and imaginary parts of  $k$ ;  $\xi_R$  and  $\xi_I$  are the real and imaginary parts of  $\xi$ . Eq. (5) is the quantum counterpart to the classical Eq. (1) with flat, perfectly reflecting surfaces ( $P = Q = 1$ ).

The KP function is used with real  $u = dk_x$  to calculate the allowed KP bands over the domain  $0 \leq k_x \leq k_F$  and to project them onto  $k_\perp$  using  $k_\perp = \sqrt{k_F^2 - k_x^2}$ , so that the integral of Eq. (5) is calculated over real domains in  $k_\perp$  which correspond to the allowed KP bands in  $k_x$ .

2.2.4. Conductivity of a thin film bounded by two flat surfaces

As shown in Appendix C, the conductivity of a thin film bounded by flat surfaces that extends from  $z = 0$  to  $z = t$  but is infinite along  $x$  and  $y$ , and contains the grains represented by Eq. (2), predicted by the quantum theory, is given by

$$\sigma = \frac{q^2}{8\pi^2 \hbar t} \sum_n \int_0^\infty \frac{I(k_n)}{|D(k_n)|^2} T_N(k_x) dk_x \quad (6)$$

where  $k_n = \sqrt{\tilde{k}_F^2 - k_y^2 - (n\pi/t)^2}$ . Again,  $T_N(k_x)$  represents the probability that the electron will be transmitted through  $N$  successive grain boundaries.  $I(k_n)$  is given by Eq. (5a) and the values of  $k_x$  lie inside the KP bands of allowed states and are such that  $k_x^2 + k_y^2 + (n\pi/t)^2 = k_F^2$ . This is the quantum counterpart to the classical Eq. (1). Details of the derivation of these formulae are included in Appendix C.

2.2.5. Effect of disorder

So far the effect of disorder has not yet been incorporated into the theory. To include the effect of disorder, let  $x_n = nd + \Delta_n$  indicate the position of the  $n$ -th grain boundary, where  $d$  is the average grain diameter and  $\Delta_n$  is a random variable such that  $\langle \Delta_n \rangle = 0$  and  $\langle \Delta_n^2 \rangle = s^2$  for  $1 \leq n \leq N$ . Let  $P_n$  be the transfer matrix relating the function  $\phi_{n-1}(x)$  representing an electron wave function for  $(n - 1)d < x < nd$ , and  $\phi_n(x)$  for  $nd < x < (n + 1)d$ . As shown in Appendix D, using the methods of an introductory course on Quantum Mechanics, we conclude

$$P_n = \begin{pmatrix} 1 + i \frac{S}{2k_x} & i \frac{S}{2k_x} \exp(-2ik_x x_n) \\ -i \frac{S}{2k_x} \exp(2ik_x x_n) & 1 - i \frac{S}{2k_x} \end{pmatrix} \quad (7)$$

As explained in Appendix D, using a Gaussian distribution of the random variable  $nd + \Delta_n$ , we obtain for the statistical average of the transfer matrix  $P_n$ :

$$P_n = \begin{pmatrix} 1 + i \frac{S}{2k_x} & i \frac{S}{2k_x} \exp(-2ik_x nd) \exp(-2k_x^2 s^2) \\ -i \frac{S}{2k_x} \exp(2ik_x nd) \exp(-2k_x^2 s^2) & 1 - i \frac{S}{2k_x} \end{pmatrix} \quad (7a)$$

Let  $M$  be the  $2 \times 2$  transmission matrix describing a carrier that traverses  $N$  barriers,  $M(N, k) = \prod_{n=1}^N P_n$ . As described in Appendix D, the probability  $T$  that the carrier traverses these  $N$  successive barriers is, approximately,  $T_N(k_x) \approx 1/|\langle M_{22}(N, k_x) \rangle|^2$ . If  $N$  is considered

as the total number of grain boundaries between the measuring contacts, then  $N \geq 10^5$  which would lead to  $T$  of order  $10^{-25}$ . A metallic film (made out of disordered nanometric grains) would never conduct electricity, on account of Anderson localization. To include the effect of disorder and yet arrive at a realistic estimation of  $T_N$  that is consistent with experimental results, we consider  $N = 1$  if  $\ell < d$ , and  $N = \text{Int}(\ell/d)$  if  $\ell > d$ , where  $\text{Int}(z)$  is the integer part of  $z$  and  $\ell$  is the temperature-dependent (unknown) electronic mean free path in the bulk. The method to compute  $T_N(k_x)$  using the morphological data describing the grain size distribution measured on each sample is discussed in Appendix D.

### 2.2.6. Contribution to the resistivity of a thin film arising from electron-rough surface scattering

To include the effect of rough surfaces limiting the film, we consider the gold-mica interface to be smooth (for the mica is atomically flat in regions extending over several hundred nm as revealed by an AFM), so we expect that the roughness that contributes mainly to the resistivity is that of the exposed gold surface. Using the Dyson equation to compute the Green's function describing the electron gas confined by a rough surface and Kubo's formalism to compute the conductivity, we calculated the self-energy of the electron gas. It is characterized by a distance  $Q$  given by [Eq. (5) from Ref. [25]]

$$Q_n(k_{\parallel}) = \frac{\xi^2 \delta^2}{2t} \pi \exp\left(-\frac{\xi^2}{4}(k_{\parallel}^2 + k_F^2)\right) \sum_n \left(\frac{n\pi}{t}\right)^2 \times \exp\left[\left(\frac{n\pi}{t}\right)^2 \frac{\xi^2}{4}\right] I_0\left(\frac{\xi^2}{2} k_{\parallel} \sqrt{k_F^2 - \left(\frac{n\pi}{t}\right)^2}\right) \quad (8)$$

where  $k_{\parallel}^2 = k_x^2 + k_y^2 = k_F^2 - \left(\frac{n\pi}{t}\right)^2$ ,  $I_0$  stands for the modified Bessel function of order zero, and the sum is performed over the filled sub bands. To include dissipation arising from electron scattering by the rough surface, we shifted the Fermi sphere (as discussed in Appendix E) by the appropriate amount, adding the appropriate imaginary component to the wave vector along  $k_z$  for each sub band.

## 3. Results

We illustrate in Fig. 1 the effect of including the KP potential arising from periodic grain boundaries separated by a distance  $d$ , projecting the allowed KP bands onto the Fermi sphere.

In Fig. 2 we compare the ratio  $\sigma/\sigma_0$  predicted by the classical and the quantum theory for samples S1, S2, where  $\sigma$  represents the conductivity of the crystalline sample containing grain boundaries, and  $\sigma_0$  is the bulk conductivity. It seems remarkable that the classical prediction approaches zero as  $\ell$  grows larger toward  $1 \mu\text{m}$ , while the quantum prediction (with  $T_N = 1$ ) approaches unity from below. The reason is, classically, the electron is partially reflected each time it collides with a grain boundary; as  $\ell$  grows larger, the number of reflecting grain boundaries increases.

In the quantum description, the effect of turning on the KP potential is simply to project onto the Fermi sphere the allowed and forbidden regions; there is no such thing as an electron partially reflected or partially transmitted through a grain boundary. As Fig. 1 illustrates, for a large bulk mean free path containing many periodically distributed grains, the decrease in conductivity – if any – when turning on the KP potential, is simply a consequence of a decrease of the number of extended electron states that are consistent with the periodicity of the grain boundaries separated by a distance  $d$  that lie on the Fermi sphere. This can be considered the proof of the assertion offered by MS – without proof – that “a periodic arrange of planes provides no resistance” (over and above the resistivity of the bulk) (Ref. [3], p. 1384). Contrary to the classical MS

theory, the decrease in conductivity with increasing  $\ell$  within the quantum theory occurs not because electrons are partially reflected at each grain boundary, but either because of a decrease of the number of extended electron states (that are consistent with the periodicity of the grain boundaries) that lie on the Fermi sphere, or because the carriers are transmitted with a probability  $T < 1$  across successive (disordered) grains, or both.

To further test the new theory, to assess its capacity to describe resistivity data and to compare the predictions of both the classical and of the quantum theory with resistivity data, it becomes necessary to estimate the unknown parameters. The quantum theory contains the unknown parameters  $\ell$  and  $R$ , the classical theory contains the additional (unknown) parameters  $P$  and  $Q$  (the reflectivity of the two surfaces limiting the film). We analyze below the temperature and thickness dependence of the resistivity of samples S1, S2, S7 and S8, using the standard temperature dependent resistivity data arising from electron-phonon scattering available for crystalline gold, following the method described in detail elsewhere to estimate these unknown parameters [4,7]. The appropriate parameters used in the analysis are listed in Table 1; the results of the resistivity data analysis are displayed in Fig. 3.

After setting  $P=0$  and  $Q=1$  in MS theory, both the classical as well as the quantum theory involve two parameters,  $R$  and  $\ell_{\text{IMP}}$ . To compare quantitatively the description of the resistivity data furnished by both theories, we use as a statistical parameter measuring the goodness of the theoretical description, the Standard Statistical Error SSE =

$$\sqrt{\frac{1}{N-2} \sum_{i=1}^N \left[ \frac{(\rho_{\text{exp}}(T_i) - \rho_{\text{theo}}(T_i))^2}{\rho_{\text{exp}}(T_i)^2} \right]}, \text{ where } \rho_{\text{exp}}(T_i) \text{ and}$$

$\rho_{\text{theo}}(T_i)$  stand for the resistivity measured (exp) and theoretically predicted (theo), respectively, at each of the  $N=20$  different temperatures  $4 \text{ K} \leq T_i \leq 300 \text{ K}$  at which the resistivity was measured on these samples (resistivity data taken from Ref. [4]). This constitutes a stringent test, for changing temperature from 4 to 300 K changes the bulk mean free path  $\ell_0$  continuously on each sample, so for each specimen we have 20 resistivity data points where the ratio  $\ell_0/t$  and  $\ell_0/d$  varies substantially. We used SSE to assess the goodness of the theoretical description, varying by  $\pm 10\%$  the parameters  $R$  and  $\ell_{\text{IMP}}$  listed in Table 1. We also explored whether or not a reflectivity  $R$  could be found in the classical theory, if we used in the classical MS formalism the value for  $\ell_{\text{IMP}}$  listed in Table 1 that is appropriate for the quantum description. The result of this comparative error analysis is listed on Table 2. Both the classical as well as the quantum theory provide a fair description of the resistivity data, for the statistical error SSE is of the order of a few percent or better.

We start the comparison with the small grained sample S1. It seems remarkable that the mean free path  $\ell_{\text{IMP}}$  attributed to impurity scattering in the classical theory can be varied by two orders of magnitude (from 3000 to 36 nm in the case of S1), and yet a reflectivity  $R$  can be found (0.410 and 0.314 for S1) that provide a comparable description of the resistivity data. Because of the wide spread use of MS theory, this came as quite a surprise to us. MS theory is supposed to provide a faithful and univocal description of the resistivity data of small grained samples, where the experiment indicates that the resistivity is, indeed, dominated by grain boundary scattering at 4 K, for the Hall mobility turns out to be proportional to the grain diameter  $d$  regardless of film thickness (Ref. [5]). The results displayed on Table 2 can be considered as evidence that the classical MS model does not discriminate properly between a resistivity arising from electron-grain boundary scattering and a resistivity arising from electron-impurity scattering, for the theory does not allow parameters ( $\ell_{\text{IMP}}$ ,  $R$ ) to be uniquely adjusted to describe the temperature dependence of the resistivity data on S1. Something similar is observed when performing the error analysis comparing the predictions of the classical MS theory and the predictions of

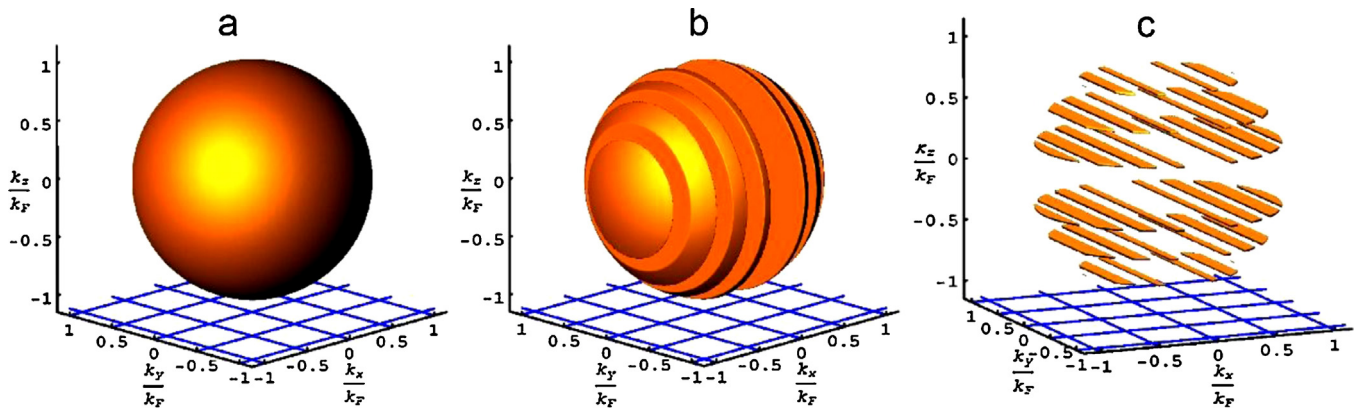


**Fig. 1.** Conducting states in a metallic specimen. (a) Colored Fermi sphere, representing the conducting states in the bulk crystalline metal. (b) Conducting states in a crystalline metal, when an array of grain boundaries represented by Eq. (2) is added to the bulk. The illustration is for the case  $dk_F = 12.1$ . (c) Conducting states in a thin metal film, when an array of grain boundaries represented by Eq. (2) is added to the film that is infinite along  $x$  and  $y$ , but limited by two flat surfaces at  $z = 0$  and  $z = t$ . The illustration is for the case  $dk_F = 12.1$  and  $t = 1$  nm.

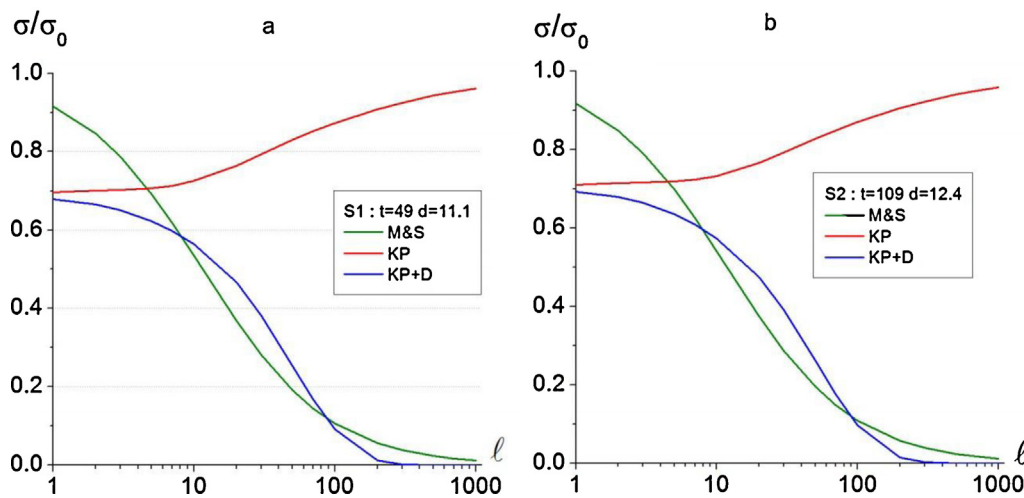


**Fig. 2.** Dependence of the ratio  $\sigma/\sigma_0$  on the bulk mean free path  $\ell$ .  $\sigma$  is the conductivity of a crystalline metal including an array of grain boundaries represented by Eq. (2),  $\sigma_0$  represents the conductivity of the bulk (in the absence of grains). Green solid line: Predictions of MS theory with  $P=Q=1$ . Red solid line: predictions of the quantum theory [Eq. (5) with  $T_N = 1$ ]. Blue solid line: predictions of the quantum theory [Eq. (5) with  $T_N < 1$ ], employing parameters listed in Table 1. (a) Predictions for sample S1. (b) Predictions for sample S2. (For interpretation of the references to color in this figure legend, the reader is referred to the web version of the article.)

the quantum theory to the temperature dependent resistivity of sample S2.

This is in contrast to the quantum theory, that provides a description of the resistivity data with a degree of goodness of the fit that is comparable to that obtained by applying the MS theory, but a 10% variation in either  $\ell_{\text{IMP}}$  or  $R$  in the quantum description induces quite a steep increase in the statistical error SSE on samples

S1 and S2. Hence the quantum theory is, indeed, capable of discriminating between a resistivity arising from electron-impurity scattering and a resistivity arising from electron-grain boundary scattering in small grained samples. The error associated to the classical description in small grained samples is comparable to the error associated to the quantum description of the resistivity data.

**Table 1**

Morphological parameters for Samples S1, S2, S7 and S8 from Ref. [4], and parameters contained in the classical theory of Mayadas and Shatzkes, and the quantum theory, needed to describe the temperature dependence of the resistivity data.

Sample	$t$ (nm)	$d$ (nm)	$s$ (nm)	Gaussian		Classical MS		Quantum		
				$\delta$ (nm)	$\xi$ (nm)	$\ell_{\text{IMP}}$ (nm)	$R$ $P=0; Q=1$	$\ell_{\text{IMP}}$ (nm)	$R$	$L_{\text{LOC}}$ (nm)
S1	49	11.1	5.3	1.3	8.9	3000	0.41	36	0.113	106
S2	109	12.4	5.3	1.3	7.3	3000	0.43	41	0.101	109
S7	54	106	43	3.1	58.4	3000	0.28	137	0.0116	19 400
S8	96	159	41	4.1	68.2	3000	0.22	295	0.0192	12 700

$t$ : film thickness;  $d$  and  $s$ : mean diameter and standard deviation of a Gaussian distribution of grains (describing the histogram of over 500 grains per sample);  $\delta$  and  $\xi$ : rms roughness amplitude and lateral correlation length describing a Gaussian roughness profile;  $\ell_{\text{IMP}}$ : mean free path (attributable to impurity scattering);  $R$ : grain boundary reflectivity, according to the MS model [Eq. (1) with  $P=0$  and  $Q=1$ ]. Parameters  $t$ ,  $d$ ,  $s$ ,  $\delta$ ,  $\xi$ ,  $R$  and  $\ell_{\text{IMP}}$  (the latter two appropriate for MS model) are taken from Ref. [4]. Rightmost three columns  $\ell_{\text{IMP}}$ : mean free path;  $R$ : grain boundary reflectivity;  $L_{\text{loc}}$ : Anderson localization length, needed to describe the resistivity according to the quantum model.

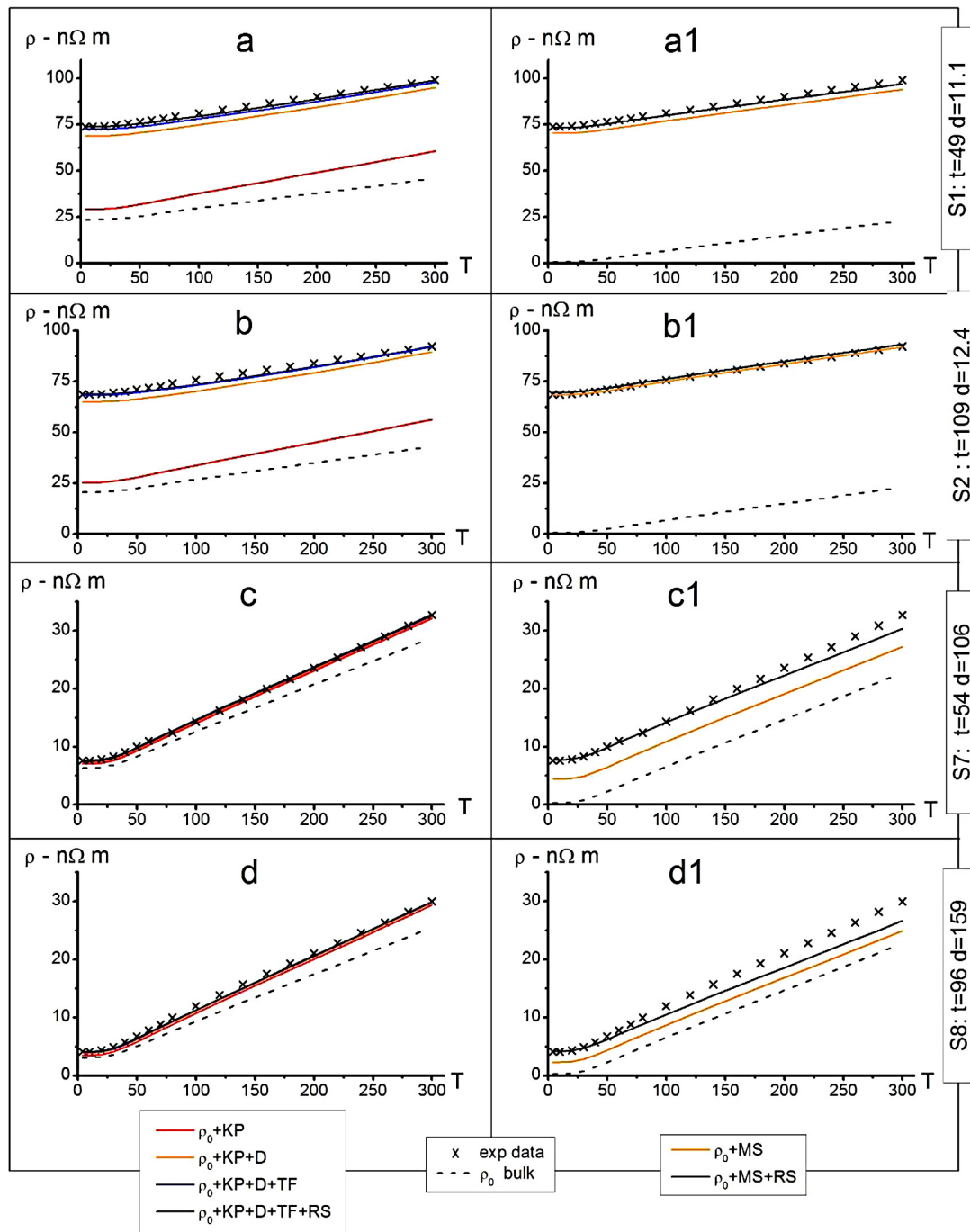


**Fig. 3.** Temperature dependence of the resistivity for samples S1, S2, S7 and S8 from Ref. [4]. (a) Crosses: experimental data, sample S1. Dashed black line:  $\rho_0$  (resistivity of the bulk), arising from electron-phonon + electron-impurity scattering, parameters listed in Table 1. Red solid line:  $\rho_0 + \text{KP}$  (Kronig–Penney) potential representing uniformly distributed grain boundaries computed from Eq. (5) with  $T_N = 1$ . Orange solid line:  $\rho_0 + \text{KP} + \text{D}$  (disorder) computed from Eq. (5) with  $T_N < 1$ . Blue solid line: resistivity of the thin film (TF)  $\rho_0 + \text{KP} + \text{D} + \text{TF}$ , computed from Eq. (6) with  $T_N < 1$ . Black solid line: resistivity of the thin film + rough surface (RS)  $\rho_0 + \text{KP} + \text{D} + \text{TF} + \text{RS}$ , the effect of the rough surface is computed from Eqs. (6) and (8) as explained in Appendix E. (a1) Crosses: experimental data, sample S1. Dashed black line:  $\rho_0$  (resistivity of the bulk). Orange solid line:  $\rho_0 + \text{MS}$ , computed from Eq. (1) with  $R$  listed in Table 1,  $P=0$ ,  $Q=1$ . (b) Resistivity of sample S2, symbols as in (a). (b1) Resistivity of sample S2, symbols as in (a1). (c) Resistivity of sample S7, symbols as in (a). (c1) Resistivity of sample S7, symbols as in (a1). (d) Resistivity of sample S8, symbols as in (a). (d1) Resistivity of sample S8, symbols as in (a1). (For interpretation of the references to color in this figure legend, the reader is referred to the web version of the article.)

In the case of large (columnar) grained sample S7 – columnar grains are the basis upon which the MS theory was built, for the grains represented by the Hamiltonian in Eq. (2) are columnar grains – a similar situation arises. The mean free path attributed to impurity scattering can be varied by a factor of 4 or larger (from 3000 to 700 nm), and yet a reflectivity  $R$  can be found (0.280 and 0.222) that provide a comparable description of the

resistivity data. Again, this is in contrast to the quantum theory, where a 10% variation in either  $\ell_{\text{IMP}}$  or  $R$  in the quantum description induces a significant increase in the statistical error SSE. A similar situation arises when the error analysis is performed comparing the resistivity predicted by the classical and quantum theory to the temperature dependent resistivity of sample S8.

**Table 2**

Comparison of the ability of the classical theory of Mayadas and Shatzkes (MS) and the quantum theory, to describe the temperature dependence of the resistivity data measured at  $N=20$  different temperatures  $4\text{ K} \leq T_i \leq 300\text{ K}$  on samples S1 and S7 (resistivity data from Ref. [4]). Both the classical MS theory and the quantum theory contain as parameters, the grain boundary reflectivity  $R$  and the mean free path  $\ell_{\text{IMP}}$  attributed to impurities/point defects. SSE stands for the standard statistical error

$$\text{SSE} = \sqrt{\frac{1}{N-2} \sum_{i=1}^N \left[ \frac{(\rho_{\text{exp}}(T_i) - \rho_{\text{theo}}(T_i))^2}{\rho_{\text{exp}}(T_i)^2} \right]}.$$

Sample	Classical MS		Quantum		SSE
	$\ell_{\text{IMP}}$ (nm)	$R$ $P=0; Q=1$	$\ell_{\text{IMP}}$ (nm)	$R$	
S1	3000	0.410			0.0162
S1	3300	0.410			0.0194
S1	2700	0.410			0.0187
S7	3000	0.370			0.156
S1	3000	0.450			0.140
S1	36	0.314			0.0180
S1	360	0.405			0.0105
S1			36	0.113	0.0138
S1			32.4	0.113	0.0241
S1			39.6	0.113	0.0384
S1			36	0.125	0.0707
S1			36	0.100	0.0859
S7	3000	0.280			0.0424
S7	3300	0.280			0.0433
S7	2700	0.280			0.0415
S7	3000	0.310			0.0533
S7	3000	0.250			0.0760
S7	137	0.00001			0.149
S7	700	0.222			0.0491
S7			136.9	0.0116	0.0136
S7			150.6	0.0116	0.0540
S7			123.2	0.0116	0.0653
S7			136.9	0.0128	0.0172
S7			136.9	0.0105	0.0148

In the case of large (columnar) grained samples S7 and S8, the error associated to the quantum description of the resistivity is about *three times smaller than the error associated to the classical description*.

#### 4. Discussion

It seems remarkable that both the MS and the quantum theory provide a fair description of the resistivity data to within a few percent and yet, the phenomena involved underlying the resistivity increase according to the MS theory and according to the quantum model are markedly different. According to the classical model, the resistivity is governed by the reflectivity  $R$  of a single grain boundary; according to the quantum theory, the resistivity is controlled by *the collective properties of an assembly of grain boundaries* (by the KP bands and by the transmission probability  $T_N$ ).

For large (columnar) grained samples where  $d > \ell(300)$  [ $\ell(300) = 38\text{ nm}$  for Au], the classical theory requires a reflectivity of about  $R = 0.22\text{--}0.28$  to explain the data, quite large for a first order perturbation theory. This is in contrast to the quantum description, where the increase in resistivity over the bulk is relatively modest, and is attributed not to partial reflection of the electrons from grain boundaries, but to *a decrease in the number of states at the Fermi sphere that are allowed bands of the KP potential; consequently, the reflectivity required turns out to be an order of magnitude smaller*.

In the opposite case of small grained samples such that  $d < \ell(300)$ , a huge  $R > 0.3$  is required by MS theory (meaning that over 30% of the electrons are reflected upon colliding with the very first grain boundary, calculated using first order perturbation theory!). This is in contrast to the quantum theory, where the increase

in resistivity arising from turning on the KP potential is relatively modest; most of the increase in resistivity over the bulk arises not from partial reflection of the electrons from grain boundaries, but is due instead to Anderson localization induced by electron scattering from successive disordered grain boundaries characterized by a localization length of the order of 110 nm. The reflectivity required by the quantum theory turns out to be about 4 times smaller than that required by the classical MS model.

The quantum description presented here exhibits yet another new and interesting feature, a strong interference between electron scattering in the bulk (B) and electron scattering by grain boundaries (GB) in a crystalline sample containing grains. In the limit of a very pure crystalline sample with a very small concentration of point defects, where the phonons are frozen out ( $\lim \ell \rightarrow \infty$ ), as stated by Thouless, the resistivity arising from electron-grain boundary scattering alone  $\rho_{\text{GB}}$  diverges as an increasing exponential of  $\ell$  with increasing bulk mean free path on account of Anderson localization. Hence, the observed resistivity of the specimen  $\rho_S$  is such that  $\rho_S \neq \rho_B + \rho_{\text{GB}}$ , where  $\rho_B$  is the resistivity of the bulk. Consequently, we expect Mathiessen's rule to be severely violated in nanometric metallic specimens made out of small grains.

#### 5. Summary

The two new elements involved in this, perhaps the simplest quantum model – a KP potential plus 1-D electron motion and electron scattering from disordered grain boundaries along a mean free path – provide a better description of the resistivity data than that furnished by the classical theory, and elucidate the physics underlying the resistivity increase over the bulk, using concepts currently accepted.

A distinctive feature of the predictions of the quantum theory is that it provides a description of the temperature dependence of the resistivity where the contribution to the resistivity originating on electron-grain boundary scattering can be described by a certain unique grain boundary reflectivity  $R$ , and the resistivity arising from electron-impurity/point defect scattering can be described by a certain unique  $\ell_{\text{IMP}}$  mean free path attributable to impurity scattering. This is in contrast to the classical MS theory, where the same temperature dependent resistivity data can be described using different sets of  $(R, \ell_{\text{IMP}})$ .

The description of the increase in resistivity provided by the quantum theory involves a change in outlook that has profound consequences. In the classical picture each grain boundary contributes to the electrical resistance by reflecting a certain fraction of the incoming electrons. In the quantum conception, there are states (in the allowed KP bands) that transmit electrons unhindered, without reflections, while the electrons in the remaining states (the forbidden KP bands) are localized. The result is that: (i) In samples where the grain diameter is appreciably smaller than the bulk mean free path at room temperature, the increase in resistivity *originates primarily from Anderson localization of electrons propagating through disordered grains*; (ii) Because of Anderson localization, *Mathiessen's rule is expected to be severely violated in small grained samples*; (iii) The increase in resistivity observed in films made out of columnar grains (where the grain diameter is larger than the electron mean free path at room temperature), originates primarily not from electrons reflected at individual grain boundaries, *but from a decrease in the number of states on the Fermi sphere that are allowed KP bands*.

The immediate practical application of the quantum theory contained in this paper resides in that we expect Anderson localization to be the dominant mechanism controlling the resistivity of metallic interconnects involved in the manufacturing of integrated circuits planned by the electronic industry worldwide (ITRS) for



the next decade. Therefore, controlling (and increasing) not only the average grain diameter but also decreasing the degree of disorder characterizing the grain size distribution, may have a significant impact in the resistivity of these nanometric interconnects.

**Acknowledgments**

We acknowledge funding from FONDECYT under contract 1120198. L. Moraga gratefully acknowledges funding from Fondo Interno de Investigacion, Universidad Central 2013 under contract UCEN 201343. R. Henriquez acknowledges funding from Proyecto Insercion CENAVA 791100037. E. Muñoz acknowledges funding from FONDECYT under contract 1141146. R. Munoz also acknowledges funding from FONDECYT under contract Anillo ACT 1117.

**Appendix A. Green’s function for the Kronig–Penney potential**

The Schrödinger equation we are interested in solving is

$$\left(-\frac{\hbar^2}{2m}\nabla^2 + V(\vec{r})\right)\psi(x, y, z) = \varepsilon_F\psi(x, y, z)$$

with the help of the Green’s function  $G(r, r') = G(r, r'; E = \varepsilon_F)$  satisfying

$$\left(\frac{\hbar^2}{2m}\nabla^2 + \varepsilon_F - V(\vec{r})\right)G(\vec{r}, \vec{r}') = \delta(\vec{r}, \vec{r}')$$

where the potential  $V(\mathbf{r})$  is given by Eq. (2).

We separate variables, so  $\Psi(x, y, z) = \phi(\xi, x)f(y, z)$  using Bloch states, with

$$\phi(\xi, x) = \sum_{m=-\infty}^{\infty} \theta_m(x)\exp(im\xi)u(x - md)$$

with  $u(x) = \sin[k(x - d)] + \exp(i\xi)\sin[kx]$  and  $\theta_m = 1$  if  $md \leq x \leq (m + 1)d$  and zero otherwise, so that

$$\phi(\xi, x) = \sum_{m=-\infty}^{\infty} \theta_m(x)\exp(im\xi)\{\sin[k(x - (m + 1)d)] - \exp(i\xi)\sin[k(x - md)]\} \tag{A.1}$$

In order that  $\phi(\xi, x)$  satisfies the potential described by Eq. (2), the parameters  $\xi$  and  $k$  must satisfy  $\cos \xi = \cos(kd) + (S/2k)\sin(kd)$ , which is Eq. (4) with  $u = kd$ .

In the case of the bulk crystal plus the Kronig–Penney potential (2),  $f(y, z)$  should be plane waves with  $k^2 = k_F^2 - k_{\perp}^2$ , where  $\mathbf{k}_{\perp} = k_y\mathbf{y} + k_z\mathbf{z}$  (where  $\mathbf{y}$  and  $\mathbf{z}$  are unit vector along  $y$  and  $z$ ). We now proceed to calculate the Fourier Transform

$$G(\vec{r}, \vec{r}') = \frac{2m}{\hbar^2} \int \frac{d^2\vec{k}_{\perp}}{4\pi^2} \exp[i\vec{k}_{\perp}(\vec{r}_{\perp} - \vec{r}'_{\perp})]g(k; x, x') \tag{A.2}$$

where  $\mathbf{r}_{\perp} = \mathbf{y}\mathbf{y} + \mathbf{z}\mathbf{z}$ , and  $g(k; x, x')$  is a one-dimensional Green’s function, satisfying

$$\frac{\partial^2 g(k; x, x')}{\partial x^2} + \left[k^2 - S \sum_n \delta(x - nd)\right]g(k; x, x') = \delta(x - x') \tag{A.3}$$

with  $k = \sqrt{k_F^2 - k_{\perp}^2}$ .

We compute  $g(k; x, x')$  from the Dyson equation:

$$g(k; x, x') = g_0(k; x, x') + \int_{-\infty}^{\infty} g_0(k; x, x_1)v(x_1)g(k; x_1, x') dx_1$$

where  $v(x) = S \sum_{n=-N/2}^{N/2} \delta(x - nd)$ .

$$g(k; x, x') = g_0(k; x, x') + S \sum_{m=-\infty}^{\infty} g_0(k; x, md)g(md, x') \tag{A.4}$$

where  $g_0(k; x, x') = \exp(ik|x - x'|)/(2ik)$  is Green’s function of a free particle. By successively putting  $x = nd$  in Eq. (A.4), we obtain a system of linear equations:

$$\sum_{m=-\infty}^{\infty} C_{n-m}g(k; md, x') = g_0(k; nd, x'); \quad n = 0, \pm 1, \pm 2, \dots \tag{A.5}$$

where

$$C_n = \delta_{n,0} - S \frac{\exp(ikd|n|)}{2ik} \tag{A.6}$$

We solve this (circulant) equation by using Fourier transforms. We denote the Fourier transform of a function  $f_n$  – depending on a discrete index  $n = 0, \pm 1, \pm 2, \dots$  ranging over an infinite interval – by  $\tilde{f}(\xi)$  and note that these are related by the Fourier theorem:

$$\tilde{f}(\xi) = \sum_{n=-\infty}^{\infty} f_n \exp(in\xi); \quad f_n(\xi) = \frac{1}{2\pi} \int_0^{2\pi} \tilde{f}(\xi) \exp(-in\xi) d\xi \tag{A.7}$$

It is seen that  $\tilde{f}(\xi + 2\pi) = \tilde{f}(\xi)$ . Alternatively, Eq. (A.7) can be stated as the pair of the well-known orthogonality and completeness relations,

$$\frac{1}{2\pi} \int_0^{2\pi} \exp(in\xi) d\xi = \delta_{n,0}; \quad \sum_{n=-\infty}^{\infty} \exp(in\xi) = 2\pi\delta(\xi) \tag{A.8}$$

By Fourier transforming  $C_n, g_0(k; nd, x')$  and  $g(k; nd, x')$ , we find that (A.5) is equivalent to the algebraic equation

$$\tilde{C}(k; \xi)\tilde{g}(k; \xi, x') = \tilde{g}_0(k; \xi, x') \tag{A.9}$$

where

$$\begin{aligned} \tilde{C}(k; \xi) &= \sum_{n=-\infty}^{\infty} C_n(k) \exp(in\xi) = 1 - \frac{S}{2ik} - \frac{S}{2ik} \sum_{n=1}^{\infty} [\exp[in(kd + \xi)] \\ &+ \exp[in(kd - \xi)]] = \frac{\cos kd + S \sin kd - \cos \xi}{\cos kd - \cos \xi} \end{aligned} \tag{A.10}$$

The series converges as long as  $\Im m(k) > 0$ . In the same way,

$$\begin{aligned} \tilde{g}_0(k; \xi, x') &= \sum_{n=-\infty}^{\infty} g_0(k; nd, x') \exp(in\xi) \\ &= \frac{1}{2ik} \sum_{n=-\infty}^{\infty} \exp[ik|nd - x'| + in\xi] = \frac{\phi(\xi, x')}{2k(\cos kd - \cos \xi)} \end{aligned} \tag{A.11}$$

where  $\phi(\xi; x)$  is given by Eq. (A.1). We note that this function obeys Bloch’s theorem. Furthermore, by using the fact that  $d\theta_m(x)/dx = -\delta[x - (m + 1)d] + \delta(x - md)$ , we can check that

$$\begin{aligned} \frac{\partial^2 \phi(\xi; x)}{\partial x^2} + \left[k^2 - S \sum_n \delta(x - nd)\right]\phi(\xi; x) \\ = 2k [\cos kd + (S/2k) \sin kd - \cos \xi] \sum_{n=-\infty}^{\infty} \delta(x - nd) \exp(in\xi) \end{aligned}$$

Clearly, only for those values of  $\xi$  such that the Kronig–Penney condition (4) is satisfied, the wave is a solution of the homogeneous Schrödinger equation. If we assume that  $\xi$  is a real angle belonging

to the interval  $0 \leq \xi < 2\pi$ , this condition can not always be satisfied. These forbidden states describe gaps that separate bands of allowed energies. Alternatively, if we allow for both  $k$  and  $\xi$  to be complex variables, we find that these forbidden states correspond to values of  $\xi$  having a large positive imaginary part with the result that, by Eq. (A.1), the wave function is strongly attenuated when propagating along the  $x$ -axis. This is used to include the effects of electron scattering by other sources, by means of a renormalization of  $k_F$  that includes a complex part.

We note further that, in case when  $\xi = \pm kd$ , the wave function describes a free particle

$$\phi(\pm kd; x) = -\exp(\pm ikx) \sin kd \quad (\text{A.12})$$

Finally, we see that  $\phi(-\xi, x)$  and  $\phi(\xi, x)$  are independent functions. (They describe, respectively, particles propagating from right to left and from left to right.) Thus, the Wronskian of these two functions is

$$W\{\phi(-\xi, x), \phi(\xi, x)\} = 2ik \sin(kd) \sin \xi \quad (\text{A.13})$$

We can now determine the one-dimensional Green's function  $g(k; nd, x')$ . By Fourier theorem

$$g(k, nd, x') = \frac{1}{2\pi} \int_0^{2\pi} \frac{\tilde{g}(k; \xi, x')}{\tilde{C}(k; \xi)} \exp(-in\xi) d\xi = \frac{1}{4\pi k} \int_0^{2\pi} \frac{\phi(\xi; x') \exp(-in\xi)}{\cos kd + (S/2k) \sin kd - \cos \xi} d\xi \quad (\text{A.14})$$

Finally, we find the desired Green's function  $g(x, x')$  by replacing this expression into Eq. (A.4),

$$g(k; x, x') = g_0(k; x, x') + \frac{S}{4\pi k} \sum_{n=-\infty}^{\infty} \int_0^{2\pi} \frac{g_0(k; x, nd) \exp(-in\xi) \phi(\xi; x')}{\cos kd + (S/2k) \sin kd - \cos \xi} d\xi$$

Now, the sum over  $n$  can be performed by appealing to (A.11). The result is

$$g(k; x, x') = g_0(k; x, x') + \frac{S}{8\pi k^2} \int_0^{2\pi} \frac{\phi(-\xi; x) \phi(\xi; x')}{(\cos kd - \cos \xi) [\cos kd + (S/2k) \sin kd - \cos \xi]} d\xi \quad (\text{A.15})$$

We note the integrand has simple poles at these values of  $\xi$  that satisfy the Kronig–Penney condition (4) besides the two extra poles at  $\xi = \pm kd$ . It is seen that, as a consequence of (A.9), the residues over these extra poles just result in  $-g_0(k; x, x')$ . The residue over the pole given by the value of  $\xi$  that satisfies  $\cos kd + (S/2k) \sin kd - \cos \xi = 0$  (for fixed  $k$ ) is the expression given by Eq. (4).

Consequently,

$$g(k; x, x') = \frac{\phi(-\xi, x) \phi(\xi, x')}{2ik \sin(kd) \sin \xi} \quad \text{if } x < x' \quad (\text{A16a})$$

$$g(k; x, x') = \frac{\phi(-\xi, x') \phi(\xi, x)}{2ik \sin(kd) \sin \xi} \quad \text{if } x > x' \quad (\text{A16b})$$

## Appendix B. Conductivity of a crystalline sample containing uniform, equally spaced grains

We use the Kubo formula (3) for calculating the electrical conductivity

$$\sigma = -\frac{2q^2 \hbar^3}{\pi m^2 \Omega} \int d^3 \vec{r} \int d^3 \vec{r}' \left[ \Im m \frac{\partial G(\vec{r}, \vec{r}')}{\partial x} \right] \left[ \Im m \frac{\partial G(\vec{r}', \vec{r})}{\partial x'} \right] \quad (\text{3})$$

By inserting into (3) Green's function for the infinite domain

$$G_0(\vec{r}, \vec{r}') = -\frac{2m}{4\pi \hbar^2} \frac{\exp(i\tilde{k}_F |\vec{r} - \vec{r}'|)}{|\vec{r} - \vec{r}'|} \quad \text{where } \tilde{k}_F \text{ is a complex quantity, one obtains, for the conductivity of a bulk sample,}$$

$$\sigma_0 = \frac{q^2 [\Re e(\tilde{k}_F)]^2}{6\pi^2 \hbar [\Im m(\tilde{k}_F)]}$$

where  $\Re e(z)$  represents the real part of the complex number  $z$ . This coincides with the well-known Sommerfeld's prescription [26]

$$\sigma_0 = \frac{q^2 k_F^2 \ell}{3\pi^2 \hbar}$$

if we identify the real part of the complex wave vector  $\tilde{k}_F$  with the value  $k_F$  of the Fermi wave vector and its imaginary part with  $\Im m \tilde{k}_F = 1/(2\ell)$ . The Kubo formula (3) simplifies considerably if written in terms of  $g$ . The result is

$$\sigma = -\frac{4q^2}{\pi^2 \hbar L} \int_{-L/2}^{L/2} dx \int_{-L/2}^{L/2} dx' \int_0^\infty k_\perp \left[ \Im m \frac{\partial g(k; x, x')}{\partial x} \right] \times \left[ \Im m \frac{\partial g(k; x, x')}{\partial x'} \right] dk_\perp \quad (\text{B.1})$$

By using the identity  $\Im m A \Im m B = (1/2) \Re e(AB^* - AB)$  we see that Eq. (B.1) can be written as

$$\sigma = -\frac{2q^2}{\pi^2 \hbar} \int_0^\infty k_\perp |I_1 - I_2| dk_\perp \quad (\text{B.2})$$

where

$$I_1 = \frac{1}{L} \int_{-L/2}^{L/2} dx \int_{-L/2}^{L/2} dx' \left[ \frac{\partial g(k; x, x')}{\partial x} \right] \left[ \frac{\partial g^*(k; x', x)}{\partial x'} \right] \quad (\text{B.3})$$

$$I_2 = \frac{1}{L} \int_{-L/2}^{L/2} dx \int_{-L/2}^{L/2} dx' \left[ \frac{\partial g(k; x, x')}{\partial x} \right] \left[ \frac{\partial g(k; x', x)}{\partial x'} \right] \quad (\text{B.4})$$

By using the particular structure of Green's function (A.16), it is seen that

$$I_2 = \frac{1}{D^2 L} \int_{-L/2}^{L/2} dx \left[ f(\xi; x) \int_{-L/2}^x f(-\xi; x') dx' + f(-\xi; x) \int_x^{L/2} f(\xi; x') dx' \right] \quad (\text{B.5})$$

where  $D = 2ik \sin(kd) \sin(\xi)$  and

$$f(\xi; x) = \phi(\xi; x) \frac{\partial \phi(\xi; x)}{\partial x} = \frac{1}{2} \frac{\partial |\phi(\xi; x)|^2}{\partial x} = \frac{1}{2} F'(\xi; x) \quad (\text{B.6})$$

Therefore,

$$I_2 = \frac{1}{4D^2 L} \int_{-L/2}^{L/2} [F'(\xi; x) F(-\xi; x) - F'(-\xi; x) F(\xi; x)] dx + B \quad (\text{B.7})$$

where

$$B = -\frac{1}{4D^2 L} \{ [F(\xi; L/2) - F(\xi; -L/2)] F(-\xi; -L/2) - [F(-\xi; L/2) - F(-\xi; -L/2)] F(\xi; L/2) \} \quad (\text{B.7a})$$

and the terms outside the integrals are of order  $N^{-1}$  and can be neglected. Thus, the integral simplifies to

$$I_2 = \frac{1}{2DL} \int_{-L/2}^{L/2} \phi(\xi; x)\phi(-\xi; x) dx \tag{B.8}$$

A similar analysis may be applied to the integral  $I_1$ . We use the identity

$$\phi(\xi; x) \frac{\partial \phi^*(\xi; x)}{\partial x} = \frac{1}{2} \frac{\partial}{\partial x} |\phi(\xi; x)|^2 + \frac{1}{2} W\{\phi(\xi; x), \phi^*(\xi; x)\} \tag{B.9}$$

where  $W\{f(x), g(x)\} = f(x) \frac{dg(x)}{dx} - g(x) \frac{df(x)}{dx}$  is the Wronskian of  $f$  and  $g$  and note that, since

$$W\{\phi(\xi; x), \phi^*(\xi; x)\} = 2i\gamma m \left[ \phi(\xi; x) \frac{\partial \phi^*(\xi; x)}{\partial x} \right] \tag{B.10}$$

the term containing the Wronskian is purely imaginary. Inserting this decomposition into the expression for  $I_1$  we find that, after dropping terms that are imaginary and thus do not contribute to the conductivity,

$$\text{Re} I_2 = I_1 + \frac{1}{4|D|^2} I(k) \tag{B.11}$$

where the integral  $I(k)$  is given by

$$I(k) = \frac{1}{L} \int_{-L/2}^{L/2} dx \left[ X(\xi; x) \int_{-L/2}^x X(-\xi; x') dx' + X(-\xi; x) \int_x^{L/2} X(\xi; x') dx' \right] \tag{B.12}$$

and we define

$$X(\xi; x) = W\{\phi(\xi; x), \phi^*(\xi; x)\} \tag{B.13}$$

We note that the Wronskian depends on  $x$  in this case since, due to dissipation,  $\psi(\xi; x)$  and  $\psi^*(\xi; x)$  do not satisfy the same Schrödinger equation.

Now, it is advantageous to introduce explicitly a primitive  $Z(\xi; x)$  of  $X(\xi; x)$  such that

$$X(\xi; x) = \frac{\partial Z(\xi; x)}{\partial x} \tag{B.14}$$

since, if we neglect again terms of the order  $N^{-1}$ , the integral can be simply written as

$$I(k) = \frac{1}{L} \int_{-L/2}^{L/2} W\{Z(-\xi; x), Z(\xi; x)\} dx \tag{B.15}$$

It follows from Eq. (A.1) that  $W\{Z(-\xi; x), Z(\xi; x)\}$  is a periodic function of  $x$  with period  $d$ . Thus,

$$I(k) = \frac{1}{d} \int_0^d W\{z(-\xi; x), z(\xi; x)\} dx \tag{B.16}$$

where  $z(\xi; x)$  is given by

$$z(\xi; x) = \frac{i}{2} \left\{ \frac{k_R}{k_I} \cosh[2k_I(x-d)] + \frac{k_I}{k_R} \cos[2k_R(x-d)] \right\} + D + E \tag{B.17}$$

$$D = \frac{i}{2} \exp(-2\xi_I) \left[ \frac{k_R}{k_I} \cosh(2k_I x) + \frac{k_I}{k_R} \cos(2k_R x) \right]$$

$$E = -i \text{Re} \left\{ \exp(i\xi) \left[ \frac{k_R}{k_I} \cos(2ik_I x + k^* d) + \frac{k_I}{k_R} \cos(2k_R x - k^* d) \right] \right\}$$

and where  $k_R$  and  $k_I$  are the real and imaginary parts of the wave vector  $\mathbf{k}$ .

The Wronskian  $W\{z(-\xi; x), z(\xi; x)\}$  can now be calculated and the integral over  $x$  performed by hand. The result is formula (5).

### Appendix C. Thin films bounded by smooth surfaces

In this section we consider the effects of grain boundaries in the electrical conductivity of a thin film of thickness  $t$ . In order to disentangle these effects from those arising from surface roughness or other surface defects, we consider first only the case of perfectly smooth boundaries. Let us suppose that the sample extends from  $z=0$  to  $z=t$  and is of infinite extent in the  $x$ - and  $y$ -directions. As in Mayadas and Shatzkes, grain boundaries are represented by a regular array of barriers oriented perpendicularly to the  $x$ -axis with the potential described by Eq. (2). The Green's function for this case is

$$G(\vec{r}, \vec{r}') = \frac{2m}{\hbar^2} \sum_{n=1}^{\infty} \int_{-\infty}^{\infty} \frac{dk_y}{2\pi} \exp[ik_y(y-y')] \phi_n(z) \phi_n(z') g(k_n; x, x') \tag{C.1}$$

where

$$\phi_n(z) = \sqrt{\frac{2}{t}} \sin\left(\frac{n\pi}{t} z\right) \tag{C.2}$$

and

$$k_n = \sqrt{\tilde{k}_F^2 - k_y^2 - \left(\frac{n\pi}{t}\right)^2} \tag{C.3}$$

As a consequence of the separability of this problem, the Green's function  $g(k_n; x, x')$  is still given by Eq. (A.16).

Proceeding as before, we find that in this case the electrical conductivity is given by

$$\sigma = \frac{q^2}{8\pi^2 \hbar t} \sum_n \int_0^{\infty} \frac{I(k_n)}{|D(k_n)|^2} dk_y$$

Again, here  $I(k)$  is given by Eq. (5a) and the values of  $k_y$  and  $n$  are restricted so that  $k_x$  lies inside the KP bands of allowed states and are such that  $k_x^2 + k_y^2 + (n\pi/t)^2 = k_F^2$ .

We extend the treatment to a wire bounded by smooth surfaces, of rectangular cross-section of dimensions  $D_y, D_z$  such that  $0 \leq y \leq D_y, 0 \leq z \leq D_z$  and very long in the  $x$ -direction. The effect of grain boundaries is, again, accounted for by means of the model of Mayadas and Shatzkes. It is seen that the appropriate Green's function is

$$G(\vec{r}, \vec{r}') = \frac{2m}{\hbar^2} \sum_{n=1}^{\infty} \sum_{m=1}^{\infty} Y_n(y) Y_n(y') Z_m(z) Z_m(z') g(k_{m,n}; x, x') \tag{C.4}$$

where

$$Y_n(y) = \sqrt{\frac{2}{D_y}} \sin\left(\frac{n\pi}{D_y} y\right); \quad Z_m(z) = \sqrt{\frac{2}{D_z}} \sin\left(\frac{m\pi}{D_z} z\right) \tag{C.5}$$

and  $g(k_{m,n}; x, x')$  is given by Eq. (A.16). Here  $k_{m,n} = \sqrt{\tilde{k}_F^2 - \left(\frac{n\pi}{D_y}\right)^2 - \left(\frac{m\pi}{D_z}\right)^2}$ .

The electrical conductivity is given by

$$\sigma = \frac{q^2}{4\pi \hbar D_y D_z} \sum_{n,m} \frac{I(k_{m,n})}{|D(k_{m,n})|^2} \tag{C.6}$$

As before,  $I(k)$  is given by Eq. (5a) and the sum is performed only over those values of  $n$  and  $m$  so that  $k_x$  lies inside the KP bands of allowed states and are such that  $k_x^2 + (n\pi/D_y)^2 + (m\pi/D_z)^2 = k_F^2$ .

#### Appendix D. Transfer matrix $P_n$ and transmission coefficient $T_N(k_x)$

In order to fill in the gap left in the work by Mayadas and Shatzkes, we use standard Quantum Mechanics to calculate the transfer matrix  $P_n$  across the boundary located at  $x_n = nd$ ,  $n \geq 1$ , where there is a grain boundary, the potential of which is represented by  $(\hbar^2 S/2m)\delta(x - nd)$  contained in the Hamiltonian [(Eq. (2))]. We represent these Bloch states by

$$\begin{aligned} \phi_{n-1}(x) &= A_{n-1} \exp(+ikx) + B_{n-1} \exp(-ikx) \quad \text{valid for } (n-1)d \leq x \leq nd \\ \text{and by } \phi_n(x) &= A_n \exp(+ikx) + B_n \exp(-ikx) \quad \text{valid for } nd \leq x \leq (n+1)d \end{aligned}$$

where  $A_{n-1}$ ,  $B_{n-1}$ ,  $A_n$  and  $B_n$  are complex coefficients. We impose the following boundary conditions which are standard for this kind of problems in an introductory course on quantum mechanics:

$$\begin{aligned} \text{(i)} \quad & \phi_{n-1}(x=x_n) = \phi_n(x=x_n) \\ \text{(ii)} \quad & -\frac{\hbar^2}{2m} \left\{ \left( \frac{d\phi_n(x)}{dx} \right)_{x=x_n} - \left( \frac{d\phi_{n-1}(x)}{dx} \right)_{x=x_n} \right\} + \frac{\hbar^2}{2m} S \phi_n(x=x_n) = 0. \end{aligned}$$

These boundary conditions lead to the following relations between the coefficients  $A$ ,  $B$ :

$$\begin{aligned} \text{(i')} \quad & A_{n-1} \exp(+ikx_n) + B_{n-1} \exp(-ikx_n) = A_n \exp(+ikx_n) + B_n \exp(-ikx_n), \\ \text{(ii')} \quad & A_{n-1} [1 + i(S/k)] \exp(+ikx_n) + B_{n-1} [i(S/k) - 1] \exp(-ikx_n) = A_n \exp(+ikx_n) - B_n \exp(-ikx_n). \end{aligned}$$

Solving for  $A_n$ ,  $B_n$  in terms of  $A_{n-1}$ ,  $B_{n-1}$ , we obtain the transfer matrix  $P_n$  described by Eq. (7), defined by  $\begin{pmatrix} A_n \\ B_n \end{pmatrix} = P_n \begin{pmatrix} A_{n-1} \\ B_{n-1} \end{pmatrix}$ .

Note that  $\det(P_n) = 1$ .

As explained in Section 2.2.5, to describe the effect of disorder, let  $x_n = nd + \Delta_n$  indicate the position of the  $n$ -th grain boundary, where  $d$  is the average grain diameter and  $\Delta_n$  is a random variable such that  $\langle \Delta_n \rangle = 0$  and  $\langle \Delta_n^2 \rangle = s^2$ ,  $\langle \Delta_n \Delta_m \rangle = \delta_{m,n} \langle \Delta_n^2 \rangle = s^2 \delta_{m,n}$  for  $1 \leq m, n \leq N$ . We assume that  $\Delta_n$  is a random variable described by a Gaussian probability density  $f(\Delta_n)$  with mean zero and standard deviation  $s^2$ ,  $f(\Delta_n) = \frac{1}{\sqrt{2\pi s^2}} \exp\left(-\frac{\Delta_n^2}{2s^2}\right)$ . We use the simplifying assumption that  $\Delta_n$ ,  $\Delta_m$ , the fluctuations in the position of the grain boundary located at  $x_n = nd$  for grains located at different sites  $n \neq m$  are *uncorrelated, and are characterized by the same mean*  $\langle \Delta_n \rangle = 0$  and the same standard deviation  $\langle \Delta_n^2 \rangle = s^2$ . Under these assumptions, we can write the transfer matrix  $M$  relating  $A_N$ ,  $B_N$  to  $A_1$ ,  $B_1$ , as  $M = P_N \times P_{N-1} \times \dots \times P_1$ , therefore the statistical average of the  $2 \times 2$  matrix  $M$  is  $\left\langle \prod_{n=1}^N P_n \right\rangle$ . Using the statistical independence

$$\text{of the random variables } \Delta_n, \Delta_m, \text{ we write } \left\langle \prod_{n=1}^N P_n \right\rangle = \prod_{n=1}^N \langle P_n \rangle.$$

Hence, the only element of the  $2 \times 2$  matrix  $P_n$  that involves the random variable  $\Delta_n$  and involves an average over an ensemble of all possible realizations of the grain size distribution, is  $i \frac{S}{2k_x} \exp(-2ik_x x_n)$ , whose statistical average is

$$\begin{aligned} & \left\langle i \frac{S}{2k_x} \exp(-2ik_x x_n) \right\rangle \\ &= i \frac{S}{2k_x} \int_{-\infty}^{\infty} f(\Delta_n) \exp[-2ik_x(nd + \Delta_n)] d\Delta_n \\ &= i \frac{S}{2k_x} \exp(-2ik_x nd) \exp(-2k_x^2 s^2) \end{aligned}$$

which is the result quoted in Eq. (7a).

To compute the transmission coefficient  $T_N$ , we write

$$A_N = M_{11}A_1 + M_{12}B_1$$

$$B_N = M_{21}A_1 + M_{22}B_1$$

and set  $B_N = 0$  for the  $N$ -th grain boundary ( $N > 1$ ), therefore  $A_N = (M_{11}M_{22} - M_{12}M_{21})/M_{22} = 1/M_{22}$ .

Finally, the transmission coefficient is, rigorously,  $T_N(k_x) = (1/|M_{22}(N, k_x)|^2)$ . Here we used as a simple estimation  $T_N(k_x) \approx 1/|\langle M_{22}(N, k_x) \rangle|^2$ .

Within this line of reasoning Anderson localization plays no role whatsoever. We stumbled on localization induced by electron scattering by successive disordered grain boundaries, after the evaluation of the transfer matrix  $P_n$  using the standard rules of Quantum Mechanics described above, and as a result of numerically evaluating  $T_N(k_x) \approx 1/|M_{22}(N, k_x)|^2$  via matrix multiplication of  $N$  matrices for each of the four samples analyzed in this work, involving  $N = 1, 2, 3, \dots$  up to 50 matrices given by Eq. (7a). These results forced us to accept localization, and to look for similar phenomena in other branches of physics. This way we arrived (at the end of this work) to Anderson localization.

Within the theory presented here, the conductivity of the specimen is proportional to the probability of transmission  $T_N(k_x, R, \ell)$  of an electron traversing  $N$  successive grain boundaries. From the argument by Thouless [17] and the work of several researchers working on Anderson localization [16,18], it is expected that the probability of transmission  $T_N(k_x, R, \ell)$  of an electron traversing  $N$  successive grain boundaries, will behave as  $T_N(k_x, R, \ell) \sim \exp[-\ell/L_{loc}(k_x, R)]$ , where  $L_{loc}(k_x, R)$  is the so-called Anderson localization length.

After accepting the fact that such numerical evaluation of  $T_N(k_x, R, \ell)$  led to Anderson's localization, we verified that  $\ln(T_N)$  is, indeed, proportional to  $-\ell$ . However, a technical difficulty arises, because of the stepwise variation of  $T_N(k_x, R, \ell)$  that necessarily occurs when a grain is added (or subtracted) from the electron trajectory because of an increasing (or decreasing) temperature dependent bulk mean free path  $\ell(T)$ . To circumvent this difficulty and to retrieve the underlying physics, we numerically computed  $T_N$  over a grid of values of  $(k_x, R)$  involving  $(100 \times 9)$  data points for each sample, using for  $t$ ,  $d$  and  $s$  the values *measured on each sample* listed in Table 1, and adjusted a smooth analytic function of  $(k_x, R)$  to the resulting  $T_N$  numerical data, seeking agreement to 7 significant figures in the neighborhood of  $k_x \approx 0.9k_F$  and  $R \approx 0.1$ , which is the region that contributes the most to the conductivity of the samples.

#### Appendix E. Contribution to the resistivity arising from electron-rough surface scattering

We use the self energy given by Eq. (8) to compute the contribution to the resistivity of a thin film arising from electron-rough surface scattering. Within the formalism used in Refs. [23,25], the wave functions describing the electron gas that extends indefinitely along  $x$  and  $y$ , but is confined by two rough surfaces at  $z = 0$  and  $z = t$ , is

$$\varphi_-(z) = \exp(-ik_z z) - A_0 \exp(ik_z z) \quad (E.1)$$

$$\varphi_+(z) = \exp(+ik_z z) - A_t \exp(2ik_z t - ik_z z)$$

where  $\varphi_-(z)$  represents the wave function propagating along  $-z$ ,  $\varphi_+(z)$  represents the wave function propagating along  $+z$ , while  $A_0$

and  $A_t$  represent the amplitude of the wave functions reflected by the rough surfaces located at  $z=0$  and  $z=t$ , respectively. In the case of these gold films,  $A_0=1$ , since AFM reveals that the mica surface is flat in regions of the order of a few hundred nm. Within the quantum formalism of Refs. [23,25],  $A_t$  is given by

$$A_t = \frac{1 - k_z Q_n(k_{\parallel})}{1 + k_z Q_n(k_{\parallel})} \quad (\text{E.2})$$

where  $Q_n(k_{\parallel})$  is given by Eq. (8). Let  $A_t = \exp(2i\delta_t)$ . Then, the one-dimensional Green's function is

$$g(k_z; z, z') = \frac{\sin(k_z z) \sin[k_z(z' - t) - \delta_t]}{k_z \sin(k_z t + \delta_t)} \quad \text{if } z < z' \quad (\text{E.3a})$$

$$g(k_z; z, z') = \frac{\sin(k_z z') \sin[k_z(z - t) - \delta_t]}{k_z \sin(k_z t + \delta_t)} \quad \text{if } z > z'. \quad (\text{E.3b})$$

The energy level of the electron gas is given by the wave vectors  $k_{z,n}$  associated with the poles of this Green's function. These poles and the corresponding wave vectors  $k_{z,n}$  are obtained by solving Eq. (E.2),

$$k_{z,n} t = n\pi - \frac{1}{2i} \ln \frac{1 - k_{z,n} Q_n(k_{\parallel,n})}{1 + k_{z,n} Q_n(k_{\parallel,n})} \quad (\text{E.4})$$

If  $\delta_t=0$ , then the Green's function describing the flat surface has poles at  $k_{z,n}(\delta_t=0) = n\pi/t$ , where  $1 \leq n \leq \text{Int}(tk_F/\pi)$ , which describe the sub bands of the electron gas confined between two parallel flat surfaces.

To determine the complex poles  $k_{z,n}$  satisfying (E.4) for the rough surface of samples S1, S2, S7 and S8, we computed  $Q_n$  according to Eq. (8) using the parameters  $(\delta, \xi)$  listed in Table 1 for each sample, and used as a first approximation to compute  $Q_n$ , the value  $k_{\parallel,n} = \sqrt{k_F^2 - (n\pi/t)^2}$ . The transcendental equation (E.4) was solved numerically for the complex  $k_{z,n}$  using a Newton–Raphson method until a precision of 10 digits was obtained for each sub band  $1 \leq n \leq \text{Int}(tk_F/\pi)$ .

To include dissipation arising from electron scattering by the rough surface, the values of  $k_{z,n}$  determined numerically were used to shift the Fermi sphere adding an imaginary part to the wave vector  $k_z$ ; the complex numerical solution of Eq. (E.4) was employed to compute the corrected values of  $k_n = \sqrt{\tilde{k}_F^2 - k_{z,n}^2 - k_y^2}$  for each sub band before performing the integration on Eq. (6).

## References

- [1] K. Fuchs, Proc. Camb. Philos. Soc. 34 (1938) 100.
- [2] E.H. Sondheimer, Adv. Phys. 1 (1952) 1.
- [3] A.F. Mayadas, M. Shatzkes, Phys. Rev. B 1 (1970) 1382.
- [4] R. Henriquez, et al., Appl. Surf. Sci. 273 (2013) 315.
- [5] R. Henriquez, et al., Appl. Phys. Lett. 102 (2013) 051608.
- [6] R. Henriquez, et al., Phys. Rev. B 82 (2010) 113409.
- [7] R.C. Munoz, et al., J. Appl. Phys. 110 (2011) 023710.
- [8] R. Henriquez, et al., J. Appl. Phys. 108 (2010) 123704.
- [9] R.C. Munoz, et al., Phys. Rev. Lett. 96 (2006) 206803.
- [10] F.J. Blatt, Theory of mobility of electrons in solids Solid State Physics, Advances in Research and Applications, vol. 4, Academic Press, 1957, pp. 199.
- [11] D. Choi, et al., J. Appl. Phys. 115 (2014) 104308.
- [12] J.M. Rickman, K. Barmak, J. Appl. Phys. 114 (2013) 133703.
- [13] S. Chatterjee, A.E. Meyerovich, Phys. Rev. B 81 (2010) 245409.
- [14] A.E. Meyerovich, Phys. Rev. B 84 (2011) 165432.
- [15] R.C. Munoz, et al., J. Phys.: Condens. Matter 15 (2003) L177.
- [16] P.W. Anderson, Phys. Rev. 109 (1958) 1492.
- [17] D.J. Thouless, Phys. Rev. Lett. 39 (1977) 1167.
- [18] See Anderson's Localization in the Seventies and Beyond, by D Thouless, or any of the other 21 chapters written by researchers working on Anderson localization in 50 Years of Anderson Localization, edited by Elihu Abrahams, World Scientific Press, 2010.
- [19] R.L. Kronig, W.G. Penney, Proc. R. Soc. Lond. Ser. A 130 (1931) 499.
- [20] R. Kubo, J. Phys. Soc. Jpn. 12 (1957) 570.
- [21] J. Rammer, Quantum Field Theory of Non-Equilibrium States, Cambridge University Press, Cambridge, 2007 (Chapter 6).
- [22] G.D. Mahan, Many-Particle Physics, second ed., Plenum, New York, 1990 (Chapter 7).
- [23] L. Sheng, D.Y. Xing, Z.D. Wang, Phys. Rev. B 51 (1995) 7325.
- [24] H.E. Camblong, P.M. Levy, Phys. Rev. Lett. 69 (1992) 2835.
- [25] R.C. Munoz, et al., J. Phys.: Condens. Matter 11 (1999) L299.
- [26] N.W. Aschcroft, N.D. Mermin, Solid State Physics, Saunders, New York, 1976 (Chapter 2).